

A new approach to materials discovery for electronic and thermoelectric properties of single-molecule junctions

David Zsolt Manrique, Qusiy Hibbeb Al-Galiby, Wenjing Hong, and Colin J. Lambert

Nano Lett., **Just Accepted Manuscript** • Publication Date (Web): 19 Jan 2016

Downloaded from <http://pubs.acs.org> on January 19, 2016

Just Accepted

“Just Accepted” manuscripts have been peer-reviewed and accepted for publication. They are posted online prior to technical editing, formatting for publication and author proofing. The American Chemical Society provides “Just Accepted” as a free service to the research community to expedite the dissemination of scientific material as soon as possible after acceptance. “Just Accepted” manuscripts appear in full in PDF format accompanied by an HTML abstract. “Just Accepted” manuscripts have been fully peer reviewed, but should not be considered the official version of record. They are accessible to all readers and citable by the Digital Object Identifier (DOI®). “Just Accepted” is an optional service offered to authors. Therefore, the “Just Accepted” Web site may not include all articles that will be published in the journal. After a manuscript is technically edited and formatted, it will be removed from the “Just Accepted” Web site and published as an ASAP article. Note that technical editing may introduce minor changes to the manuscript text and/or graphics which could affect content, and all legal disclaimers and ethical guidelines that apply to the journal pertain. ACS cannot be held responsible for errors or consequences arising from the use of information contained in these “Just Accepted” manuscripts.



1
2
3
4
5
6
7
8
9
10
11
12
13
14
15
16
17
18
19
20
21
22
23
24
25
26
27
28
29
30
31
32
33
34
35
36
37
38
39
40
41
42
43
44
45
46
47
48
49
50
51
52
53
54
55
56
57
58
59
60

A new approach to materials discovery for electronic and thermoelectric properties of single- molecule junctions

David Zsolt Manrique^{†,}, Qusiy Al-Galiby[†], Wenjing Hong^{‡,§}, Colin J. Lambert[†]*

[†] Department of Physics, Lancaster University, Lancaster LA1 4YB, United Kingdom

[‡] Department of Chemical and Biochemical Engineering, College of Chemistry and Chemical
Engineering, Xiamen University, Xiamen 361005, China

[§] Department of Chemistry and Biochemistry, University of Bern, Freiestrasse 3, CH-3012
Bern, Switzerland

KEYWORDS. Single molecular junction, quantum circuit, thermopower, conductance,
asymmetric and symmetric junctions, thermoelectricity

ABSTRACT. We have investigated a large set of symmetric and asymmetric molecules to
demonstrate a general rule for molecular-scale quantum transport, which provides a new
route to materials design and discovery. The rule states “the conductance G_{XBY} of an
asymmetric molecule is the geometric mean of the conductance of the two symmetric
molecules derived from it and the thermopower S_{XBY} of the asymmetric molecule is the
algebraic mean of their thermopowers”. The studied molecules have a structure X-B-Y,
where B is the backbone of the molecule, while X and Y are anchor groups, which bind the
molecule to metallic electrodes. When applied to experimentally-measured histograms of

1
2
3 conductance and thermopower, the rules apply to the statistically-most-probable values. We
4 investigated molecules with anchors chosen from the following family: cyano, pyridyl,
5 dihydrobenzothiol, amine and thiol. For the backbones B, we tested fourteen different
6 structures. We found that the formulae $(G_{XBY})^2 = G_{XBX} * G_{YBY}$ and $S_{XBY} = (S_{XBX} + S_{YBY})/2$ were
7 satisfied in the large majority of the cases, provided the Fermi energy is located within the
8 HOMO-LUMO gap of the molecules. The circuit rules imply that if measurements are
9 performed on molecules with n_A different anchors and n_B different backbones, then properties
10 of $n_A(n_A+1)n_B/2$ molecules can be predicted. So for example, in the case of 20 backbones
11 and 10 anchors, 30 measurements (or reliable calculations) can provide a near quantitative
12 estimate for 1070 measurements of other molecules, no extra cost.
13
14
15
16
17
18
19
20
21
22
23
24
25

26 Nowadays there exist a variety of techniques for measuring the electrical conductance G and
27 thermopower S of single molecules, such as scanning tunneling microscopy (STM)^{1,2}, current
28 probe atomic force microscopy^{3, 4}, STM-break junction (STM-BJ)⁵⁻⁷, crossed-wire
29 geometry⁸, nanoparticle junctions^{9, 10}, mechanically controlled break junctions(MCBJ)¹¹,
30 electromigration setups^{12,13} and nanopores¹⁴. Schematically, the measured systems are of the
31 form electrode-X-B-Y-electrode, where X and Y are anchor groups, which bind the molecule
32 to the electrodes and B is the functional backbone of the molecule. A number of experimental
33 and theoretical studies demonstrated that useful electronic and thermoelectric functionalities,
34 such as switching, sensing, rectifying and heat-to-electricity converters can be optimised by
35 modifying the backbone B of the molecules, as well as the anchors¹⁵⁻¹⁸. For molecules of
36 length less than approximately 3 nm, charge transport has been shown to be dominated by
37 phase coherent electron transport¹⁹, and therefore the subparts X, B and Y cannot be assigned
38 their own conductance or thermopower within the molecule. Nevertheless a recent
39 experimental and theoretical study demonstrated that for molecules containing serially
40 connected meta, para or ortho phenyl rings, their conductances obtained by changing the
41
42
43
44
45
46
47
48
49
50
51
52
53
54
55
56
57
58
59
60

sequencing of the rings are related to each other²⁰, which implies that molecular subparts X, B and Y are individually characterizable by single numbers. These ‘circuit rules’ provide a theoretical basis for the systematic categorisation of trends in single-molecule measurement data. They provide guidance for the design and synthesis of molecular devices with optimal electronic and thermoelectric properties by treating molecular components as individual building blocks. In this letter we show that this rule is much more widely applicable than initially suggested in ref.²⁰ and can be applied to a very wide range of symmetric and asymmetric molecules, with or without donor and/or acceptor groups. For the first time we also provide a circuit rule for the thermopower S (i.e. Seebeck coefficient) of single molecules. These circuit rules are of interest, because they provide rules for the discovery of new materials by predicting electronic and thermoelectric properties of molecules. This is particularly important, because theoretical methods such as density functional theory and GW many body theory do not usually provide quantitative predictions of such properties²¹.

It is well known that the transmission coefficient of two serially-connected phase-coherent scatterers with individual transmission coefficients T_1 and T_2 , is of the form $T = \frac{T_1 T_2}{1 - 2\sqrt{R_1 R_2} \cos \varphi + R_1 R_2}$, where φ is a quantum phase arising from quantum interference (QI) between the scatterers²². Consequently the transmission coefficient T cannot normally be factorized to a product of terms associated with the individual scatterers alone. Nevertheless, the following argument leads us to a ‘circuit rule’ which describes how the transmission changes when the sequential order of the scatterers is changed. First we note that Dyson’s equation for the Green’s function of a structure comprising three serially-connected subsystems X, B, Y is of the form

$$\begin{bmatrix} E - H_X & -V_X & 0 \\ -V_X^\dagger & E - H_B & -V_Y \\ 0 & -V_Y^\dagger & E - H_Y \end{bmatrix} \begin{bmatrix} G_{XX} & G_{XB} & G_{XY} \\ G_{BX} & G_{BB} & G_{BY} \\ G_{YX} & G_{YB} & G_{YY} \end{bmatrix} = I,$$

where H_X (H_Y) is the Hamiltonian of the combined left electrode and anchor X (right electrode and anchor Y) and V_X (V_Y) is the coupling between the backbone of the molecule and the anchor X (Y). From this expression, the relevant sub-matrix of the Green's function that describes electron propagation across the molecule from X to Y is

$$G_{YX} = g_Y V_Y^\dagger G_{BB} V_X^\dagger g_X \quad (1)$$

where $G_{BB} = (E - H_B - \Sigma)^{-1}$ is the Green's function of the coupled backbone and g_X (g_Y) is the Green's function of the combined left electrode and anchor X (right electrode and anchor Y) and $\Sigma = V_X g_X V_X^\dagger + V_Y^\dagger g_Y V_Y$. If the electrodes are coupled to the anchors through a single site at both ends, the transmission coefficient through the molecule from one electrode to the other is $T_{XBY} = (\hbar v)^2 |G_{YX}|_{ij}^2$, where v is the group velocity of the electrodes, i and j denote the anchor sites connected to electrodes^{21,23}. For molecules such as those shown in figure 1, the anchors are linked to only single sites k, l in the backbone, in which case the transmission coefficients takes the form

$$T_{XBY} = \hbar v \left| [g_Y V_Y^\dagger]_{ik} \right|^2 \left| [G_{BB}]_{kl} \right|^2 \hbar v \left| [V_X^\dagger g_X]_{lj} \right|^2 = A_Y \times B_B \times A_X, \quad (2)$$

where $A_X = \hbar v \left| [V_X^\dagger g_X]_{lj} \right|^2$, $A_Y = \hbar v \left| [g_Y V_Y^\dagger]_{ik} \right|^2$ and $B_B = \left| [G_{BB}]_{kl} \right|^2$. The factor B_B depends on X and Y via the self-energies $V_X g_X V_X^\dagger$ and $V_Y^\dagger g_Y V_Y$. However if the couplings are sufficiently weak and the Fermi energy does not coincide with the poles of g_X and g_Y , then Σ can be negligible²¹ and from eq. (2) it follows that

$$T_{XBY}^2 = T_{XBX} T_{YBY} \quad (3)$$

The dependency of B_B of X and Y is the smallest when the Fermi energy is located far away from the poles of g_X and g_Y , which is the case for off-resonant electron transport in the co-

1
2
3 tunneling regime. Based on the Landauer formula, and since eq. (3) is valid for a range of
4
5 energies larger than $kT=25$ meV, the room temperature conductance also satisfies
6
7

$$8 \quad G_{XBY}^2 = G_{XBX}G_{YBY} \quad (4)$$

9
10
11 Since this approximate relation is true for a range of energies within the HOMO-LUMO gap,
12
13 the rules for the derivatives of the logarithm of the transmission coefficients are expected to
14
15 satisfy $\frac{d}{dE} \log T_{XBY}^2 = \frac{d}{dE} \log T_{XBX} + \frac{d}{dE} \log T_{YBY}$, which leads the circuit rule for the low-
16
17 temperature thermopower²⁴:
18
19

$$20 \quad 2S_{XBY} = S_{XBX} + S_{YBY} \quad (5)$$

21
22
23 Although density functional theory (DFT) is not a quantitative theory, it has been shown to
24
25 correctly predict trends in transport properties. In order to demonstrate that the above rules
26
27 are valid for a wide range of molecular junctions, we performed DFT-based electron transport
28
29 calculations for 193 molecules. The molecules are classified according to their backbone
30
31 structures, and their attached anchors (as shown in Figure 1a,b,c). In Figure 1, X and Y
32
33 indicates the location of the anchor groups. The anchor groups X and Y are chosen from the
34
35 family CN, Py, BT, NH₂, S, several of which have been studied extensively in the literature²⁵⁻
36
37 ³². In Figure 1a, shows 180 molecules formed from 12 backbones and five anchor groups. In
38
39 the case of the 10 X-R-Y molecules shown in Figure 1b, X and Y are chosen to be one of
40
41 CN, PY, NH₂, S and in the case of the 3 X-But-Y molecules shown in Figure 1c, X and Y are
42
43 chosen to be either S or NH₂. Figure 1a,b illustrates the anchor as well as the aromatic rings,
44
45 to which the anchor is attached. For transport calculations, the planar conformations of the
46
47 molecules were considered, and the gold leads were attached perpendicularly to the plane of
48
49 the molecules as discussed in the Methods section. Examples of transmission curves for a
50
51 selection of molecules are shown in Figure 2.
52
53
54
55
56
57
58
59
60

1
2
3 The circuit formulae are first verified by calculating the room temperature conductance and
4 thermopower, using the DFT predicted Fermi energies for all molecules. To demonstrate the
5 circuit rule for conductance, we separately computed the electrical conductances (G_{XBY} ,
6 G_{XBX} , G_{YBY}) and Seebeck coefficients (S_{XBY} , S_{XBX} , S_{YBY}) of the individual molecules and
7 then plotted the square root of the product $\sqrt{G_{XBX}G_{YBY}}$ versus G_{XBY} . In Figure 3a, the small
8 scatter about a straight line demonstrates that in the majority of the cases the circuit rule gives
9 an accurate prediction for the conductance. To demonstrate the circuit rule for thermopower,
10 we separately computed the Seebeck coefficients (S_{XBY} , S_{XBX} , S_{YBY}) and then plotted the
11 average $(S_{XBX} + S_{YBY})/2$ versus S_{XBY} , as shown in Figure 3b. This remarkable result means
12 that from measurements of the conductances G_{XBX} , G_{YBY} it is possible to predict the
13 conductance G_{XBY} and similarly for the Seebeck coefficients.
14
15
16
17
18
19
20
21
22
23
24
25
26
27

28 We now discuss the sources of deviations from the circuit rule predictions. The inset of
29 Figure 3a, shows that in a number of cases a slight systematic deviation can be observed. The
30 origin of these deviations is illustrated by Figure 2, which shows several different
31 transmission coefficient curves of the X-D₁-Y type molecules. These show that if the
32 resonances of the two symmetric molecules are close to each other, then the circuit rule is
33 accurate over almost the whole of HOMO-LUMO gap; for example in Figures 2a,b, the
34 dashed purple curves compare well with the black curves. In these cases $V_X g_X V_X^\dagger \approx V_Y^\dagger g_Y V_Y$,
35 therefore even if B_B depends strongly on the self energy terms, both sides of the eq. (3)
36 follow the same energy dependence. On the other hand, if the location of the resonances of
37 X-B-X and Y-B-Y differ significantly (from Figure 2c to 2h), the error in circuit rule for the
38 transmission coefficient is large. In particular cases, when transport through one anchor (such
39 as X=NH₂) is HOMO dominated, whereas the other anchor (such as Y=Py) is LUMO
40
41
42
43
44
45
46
47
48
49
50
51
52
53
54
55
56
57
58
59
60

1
2
3 dominated, but their HOMO-LUMO gaps are similar, then the two self energy terms $V_X g_X V_X^\dagger$
4
5 and $V_Y^\dagger g_Y V_Y$ are expected to be very different. Such examples can be seen in Figures 2g,h.
6
7

8
9 We also note that the errors in circuit rule predictions for the thermopower are not necessarily
10 correlated with those of the conductance. While the magnitude of transmission coefficients is
11 inaccurate, the slope of the transmission curve of the X-D₁-Y in the log plot in Figure 2g,h
12 (black curve) remains comparable with the slope of the ones obtained with the circuit rule
13 (dashed purple). In general, Σ is the smallest and the circuit rule is most accurate when the
14 Fermi energy is furthest from both the HOMO and LUMO resonances. We note that the DFT
15 calculations typically significantly underestimate the HOMO-LUMO gap³³⁻³⁵, therefore for
16 realistic electronic structures the circuit rule may applicable even more accurately than shown
17 in Figure 2 and Figure 3. Other possibilities, that may hinder the accuracy of the circuit rules
18 for realistic conductances, are thermal fluctuations of the molecular conformation and the
19 experimental distributions of junction geometries³⁶.
20
21
22
23
24
25
26
27
28
29
30
31
32

33
34 To facilitate the utilisation of the above circuit rules for single-molecule-junction materials
35 discovery, we note that they are a consequence of the fact that the transmission coefficients
36 T_{XBY} can be factorized into a product of the kind $A_X B_B A_Y$, where A_X and A_Y do not depend
37 on B, but B_B may depend on X and Y. Nevertheless when the Fermi energy is located in the
38 valley of the HOMO-LUMO gap it is possible that Σ is negligible and therefore B_B depends
39 only on connectivity and is independent of the choice of the anchor groups. Typically if this
40 is the case, the transmission coefficients can be factorized to independent factors of anchors
41 and backbones, and these factors are transferable between different molecules. In other word,
42 the logarithm of the conductance and the thermopower are sums of transferable factors. To
43 verify this factorizability, we now assume that computed logarithmic conductance values and
44 thermopower values can be written
45
46
47
48
49
50
51
52
53
54
55
56
57
58
59
60

$$\log_{10} \frac{G_{\text{XBY}}}{G_0} = a_X + b_B + a_Y \quad (6)$$

$$\frac{S_{\text{XBY}}}{k_B/e} = a'_X + b'_B + a'_Y \quad (7)$$

where the factors $a_X, b_B, a_Y, a'_X, b'_B, a'_Y$ are independent and transferable. To obtain these parameters, we minimize numerically the function $F = \sum_B^{\text{Backbones}} \sum_X^{\text{Anchors}} \sum_{Y \geq X}^{\text{Anchors}} \left(a_X + b_B + a_Y - \log_{10} \frac{G_{\text{XBY}}}{G_0} \right)^2$, where the G_{XBY} values are the DFT-computed conductance values (see Methods section). We note that the separation between the anchor and backbone terms is arbitrary, therefore we set the backbone term of X-RR-Y type molecules to zero, i.e. we choose $b_{\text{RR}} = 0$, and in this calculation we choose the molecules in Figure 1a only. With this choice the a_X terms parametrize the anchoring structures shown in Figure 1a and Table 1, that is the anchor plus the aromatic ring. Consequently the b_B terms parametrize the backbone, that is the inner part of the molecules between the aromatic rings in Figure 1a. From $n_A=5$ different anchors and $n_B=12$ different backbones, this procedure yields 5 a_X parameters and 12 b_B parameters, from which we can reproduce the logarithmic conductance of $n_A(n_A+1)n_B/2=180$ molecules. Similarly, the same minimizing procedure is used to obtain the thermopower parameters a'_X and b'_B . Table 1 shows the anchor and backbone parameters obtained using the above minimizing procedure. To demonstrate that they can be used to predict conductances and thermopowers, Figure 4a shows a comparison between the sum $a_X + b_B + a_Y$, and the conductance G_{XBY} while Figure 4b compares $a'_X + b'_B + a'_Y$ with S_{XBY} . In Figure 4a, for each molecule, for the DFT computed conductance value G_{XBY} on the horizontal axis, we plotted the corresponding $10^{a_X+b_B+a_Y}G_0$ value marked by a red cross. The fact that the majority of the red crosses are close to the diagonal black line shows that the 5 a_X parameters and 12 b_B parameters in Table 1 can reproduce the logarithmic conductance of the 180 molecules in figure 1a accurately. In essence, by minimizing the function F with

1
2
3 respect to the 5 a_X parameters and 12 b_B parameters, we obtain their optimal value which
4
5 holds the information of the conductance values of the 180 molecules. This is possible only
6
7 because the conductance can be factorized with good accuracy according to eq. (3) and
8
9 therefore the 180 molecular conductances are not independent. Similarly, in Figure 4b, for
10
11 each molecule, for the DFT computed thermopower value S_{XBY} on the horizontal axis, we
12
13 plotted the corresponding $(a'_X + b'_B + a'_Y)S_0$ value marked by a red x. It is interesting to
14
15 note that for the conductance, the values of anchor parameter a_X in Table 1 vary less than the
16
17 values of the backbone parameters b_B . This is in contrast with the thermopower, for which
18
19 the magnitudes of the anchor parameters a'_X vary more than the magnitudes of the backbone
20
21 parameters b'_B , which suggests that the anchor may play a more dominant role in controlling
22
23 the thermopower than the conductance.
24
25
26

27
28 Having demonstrated the validity of the circuit rules, within a consistent set of DFT-based
29
30 calculations, we now discuss how they can be used experimentally for real-world discovery
31
32 of single-molecule junction properties. Although DFT is widely used for analysing electron
33
34 transport in single molecule junctions, it is at best a qualitative theory and therefore for
35
36 accurate utilisation of the rules, the parameters a_X, b_B, a_Y and a'_X, b'_B, a'_Y should be
37
38 determined experimentally. In a typical break junction experiment, the measured value of
39
40 G_{XBY} varies markedly from measurement to measurement, because of variability in the
41
42 atomic arrangement of the electrodes and in the electrode-anchor group binding geometry.
43
44 Consequently many (often thousands) of conductance measurements are made and
45
46 histograms of the logarithmic conductance $g_{XBY} = \log_{10} G_{XBY}/G_0$ are constructed. If \bar{g}_{XBY}
47
48 is the most probable value of such a histogram, then the experimentally-quoted value is
49
50 $\bar{G}_{XBY}/G_0 = 10^{\bar{g}_{XBY}}$. This variability is reflected in the anchor parameters a_X, a_Y . Therefore
51
52 when applying the circuit rule to such experiments, it should be applied in a statistical sense.
53
54
55
56
57
58
59
60

1
2
3 If the most probable values of a_X, a_Y are \bar{a}_X, \bar{a}_Y , then the most probable value of $\log_{10} \frac{G_{XBY}}{G_0}$ is
4
5
6 $\bar{g}_{XBY} = \bar{a}_X + b_B + \bar{a}_Y$. Conversely, when the fitting procedure of equation (5) in ‘Methods’ is
7
8 carried out using experimentally-quoted values, the resulting parameters are $\bar{a}_X, b_B, \bar{a}_Y$, rather
9
10 than a_X, b_B, a_Y . This is another reason why it is unsafe to use DFT values to make
11
12 quantitative predictions, because it is usually much too expensive to simulate conductance
13
14 histograms and therefore typically conductances of only a few anchoring configurations are
15
16 reported.
17

18
19 At present we are aware of only one set of measurements on both asymmetric (X-B-Y) and
20
21 symmetric (X-B-X and Y-B-Y) molecules with the same backbone. In ref ³⁷ the measured
22
23 conductance values of molecules S-R-S, NH₂-R-NH₂ are found to be $0.012G_0, 0.005G_0$
24
25 respectively and for the asymmetric NH₂-R-S molecule two conductance values $0.006G_0$ and
26
27 $0.009G_0$ were reported. The circuit rule gives $G/G_0 = 0.008$, which compares well with both
28
29 of the measured values, thereby providing a direct experimental verification of the circuit
30
31 rule. To illustrate how the circuit rules can be used to predict experimental conductances for
32
33 future molecules from measured values of molecules available in the literature, we make use
34
35 of the above factorisation procedure. To perform the fitting, we collected measured
36
37 conductances for 19 different molecules from the literature ^{20, 25, 31, 38-40} and used these to
38
39 characterize 5 anchors and 5 backbones. In Table 2 the anchor and backbone parameters are
40
41 listed characterized with the experimental conductances. The parameters obtained from the
42
43 experimental values are smaller than the theoretical values, as expected, due to the DFT’s
44
45 systematic errors with underestimating the HOMO-LUMO gap^{35, 41} and the neglect of
46
47 environmental and thermal effects in the calculations³⁶. Figure 4a and Table 3 show that the
48
49 characterisation can reproduce the conductance of the 19 different molecules with good
50
51 accuracy (marked with green triangles). The selection covers the typical experimental range
52
53 of conductances from $10^{-2}G_0$ to $10^{-6}G_0$. Usually the short molecules with higher conductance,
54
55
56
57
58
59
60

1
2
3 due to the snap back effect in the break-junction methods, are difficult to measure reliably.
4
5 The longer molecules with lower conductances (below $10^{-6} G_0$), due to the instrumental
6
7 sensitivity, are also difficult to measure. The X-T_n-X type molecules are from ref⁴⁰, where X
8
9 = Py, NH₂, S, BT and CN, and n=1,2 and 4, but varies for different X because not all
10
11 molecules could be synthesized. The conductances for the Py-OPE-Py and Py-OPE(Meta)-
12
13 Py type molecules are from ref²⁰ (Py-OPE(Meta)-Py denotes pmp), for the molecule NH₂-
14
15 OPE-NH₂ is from ref³⁹ and S-OPE-S molecule is from ref²⁶. From ref²⁹ we obtained the
16
17 conductance of NH₂-RR-NH₂ and from ref³¹ Py-RR-Py. The precise conductance values used
18
19 in the calculations are quoted in Table 3. Finally we note that in Figure 4a, the green
20
21 triangles, and Table 2, 3 and 4 are based on experimental conductance values, which
22
23 naturally includes the effect of fluctuations. The fact that the green triangles are close to the
24
25 diagonal demonstrates that the circuit rule indeed applies to 19 different experimentally-
26
27 quoted most-probable conductances.
28
29
30
31

32
33 In conclusion, we have demonstrated that for a large variety of molecules of the type X-B-Y
34
35 with different backbones B and anchors X,Y, the molecular conductance and thermopower of
36
37 asymmetric molecules can be obtained as geometric and algebraic averages of the zero-bias
38
39 conductances and thermopowers of their symmetric counterparts respectively. At a
40
41 fundamental level, a requirement for the validity of this ‘circuit rule’ is that the parts X, B
42
43 and Y should be weakly coupled, so that multiple scattering effects contained in the self-
44
45 energy Σ in equation (1) can be neglected. This also requires that the Fermi energy should be
46
47 located within the HOMO-LUMO gap of the molecules and therefore transport should be
48
49 ‘off-resonance’ and take place via coherent tunnelling. The validity of this circuit rule is
50
51 demonstrated through DFT calculations on 193 molecules, which confirms that the rule
52
53 applies to molecules exhibiting off-resonance transport. In our experience of comparing
54
55 theory with measurements of single-molecule electron transport, we have found that in
56
57
58
59
60

1
2
3 almost all cases, unless an electrostatic or electrochemical gate is applied, transport does not
4
5 take place near resonances and therefore the rule can be expected to have wide applicability.
6
7 The derivation of the rule assumes that transport takes place via coherent tunneling and that
8
9 inelastic effects are negligible. Experiment demonstrates that the length scale for the onset of
10
11 significant inelastic scattering at room temperature can be of order $3\text{nm}^{19, 42}$. All the
12
13 molecules in our study are shorter than this length. Furthermore comparison with 19
14
15 experimental molecular conductance values from the literature, originating from different
16
17 laboratories shows that the circuit rules can be applied successfully at room temperature.
18
19 Finally we note that as demonstrated in refs^{43, 44} the backbone contribution B_B (see eq. (2))
20
21 depends on the points of contact k, l of the anchors to the backbone and therefore the circuit
22
23 rule should be applied only to families of molecules containing backbones with the same
24
25 connectivity to the anchors or equivalently, backbones with different connectivities should be
26
27 treated as distinct entities, which means for example that a meta-connected backbone is
28
29 distinct from a para-connected backbone as values of b_B of OPE and OPE(meta) show in
30
31 Table 2.
32
33
34
35
36

37 For a workable thermoelectric device one needs to increase both the Seebeck coefficient S
38
39 and the electrical conductance G and simultaneously minimise the thermal conductance. The
40
41 proposed circuit rule addresses the first two challenges by predicting S and G of hitherto
42
43 unsynthesized molecules, thereby avoiding unnecessary synthetic effort. The rule also
44
45 provides new insight and chemical intuition by organising a large body of information. The
46
47 utility of the rule for ‘materials discovery’ derives from the potential translation of single-
48
49 molecule functionality into thin molecular films, formed from a monolayer of molecules is
50
51 sandwiched between a planar bottom electrode and a planar top electrode, in which the
52
53 current/heat flows through the molecules from the bottom to the top electrode. The question
54
55 of how single-molecule properties translate into thin films is non-trivial and beyond the scope
56
57
58
59
60

of this paper. However knowledge of transport properties at the single molecule level will surely inform our understanding of such thin-film materials.

For other properties, the rules can be used to obtain inequalities. For example, they imply that if S_{XX} and S_{YY} have the same sign then the powerfactor $P_{XY} = G_{XY}S_{XY}^2$ is bounded by the power factors of the symmetric molecules, that is $P_{YY} \leq P_{XY} \leq P_{XX}$ and if S_{XX} and S_{YY} have opposite sign, the powerfactor will be diminished significantly. To aid utilisation of the rules for the discovery of new junction properties, we also demonstrated that conductances and thermopowers can be characterized by transferable anchor and backbone parameters. Such characterization can be used to identify optimally functioning molecular devices for future synthesis. The accuracy of this characterization was demonstrated using experimental conductances of 19 different molecules from the literature.

Methods. In order to demonstrate computationally the circuit formulas, we performed DFT based electron transport calculations on systematically constructed gold-molecule-gold systems. All together 193 molecules were constructed with attached gold pyramids as electrodes, with anchors and backbones showed in Figures 1a,b,c. To consistently attach the pyramids to the molecules with many different backbones and anchors, we first prepared a relaxed molecular geometry with their planar and extended conformations. The relaxation was performed with MOPAC2012 RHF method and PM7 parameter-set⁴⁵ with constraints that kept the molecular conformations planar. During the relaxation, the non-hydrogen atoms were allowed to move only in the molecular plane and only the hydrogen atoms were allowed to move away from the molecular plane. The initial conformation for the relaxation was linear extended where the anchors are at the two far ends of the molecule modelling a possible conformation within an break-junction experiment (shown in Figure 5a) when a typical conductance plateau is recorded^{27, 46}. This is typically occurring when the gap between the electrodes is slightly less than the molecular length, illustrated in Figure 5a. In

the case of thiol, the sulphur was capped with a hydrogen atom for the relaxation, then after the relaxation the hydrogen atom from the sulphur was removed. We performed relaxations with SIESTA⁴⁷ DFT code (force tolerance = 0.01, GGA, DZP) as well for a few molecules and found that planar conformations are usually stable, with significant exceptions of X-RR-Y type molecules, where the aromatic rings are twisted away from each other. Since our investigation focuses on the electronic structures, we consistently kept the all structures planar. For the planar molecular structures a 35-atom 111 directed gold pyramid was attached to the anchoring atoms (S and N) perpendicularly to the molecular plane. The apex gold atom-anchor atom distance was set 2.1Å for the Py, CN anchors, 2.3Å for the NH₂ and BT and 2.35Å for the thiol anchor. This setup allowed consistent systematic comparisons between molecules with different backbones and anchors. The electronic transport calculations were performed by first obtaining the Hamiltonian of the isolated Au-molecule-Au structure by SIESTA, DZP basis set and GGA-PBE exchange-correlation potential parameterization. Then the obtained Hamiltonian was used in GOLLUM⁴⁸, with wide-band approximation to calculate the transmission coefficients, the room temperature conductance and the room temperature thermopower with the DFT computed Fermi energy. The wide-band lead was attached to the two outer layers of the gold pyramid with $\Gamma = 4.0eV$ coupling⁴⁹. The anchor and backbone parameters were determined by minimizing numerically the function

$$F = \sum_{\text{B}}^{\text{Backbones}} \sum_{\text{X}}^{\text{Anchors}} \sum_{\text{Y} \geq \text{X}}^{\text{Anchors}} \left(a_{\text{X}} + b_{\text{B}} + a_{\text{Y}} - \log_{10} \frac{G_{\text{XBY}}}{G_0} \right)^2 \quad (5)$$

with respect to the various $a_{\text{X}}, b_{\text{B}}$ parameters with the constraint $b_{\text{RR}} = 0$, using Broyden-Fletcher-Goldfarb-Shanno (BFGS) method, where 'Backbones' and 'Anchors' are in figure

1
2
3 1a, G_{XBY} is the DFT-computed conductance value and $Y \geq X$ denotes the exclusion of the
4
5 double counting the same molecule.
6
7

8 FIGURES
9

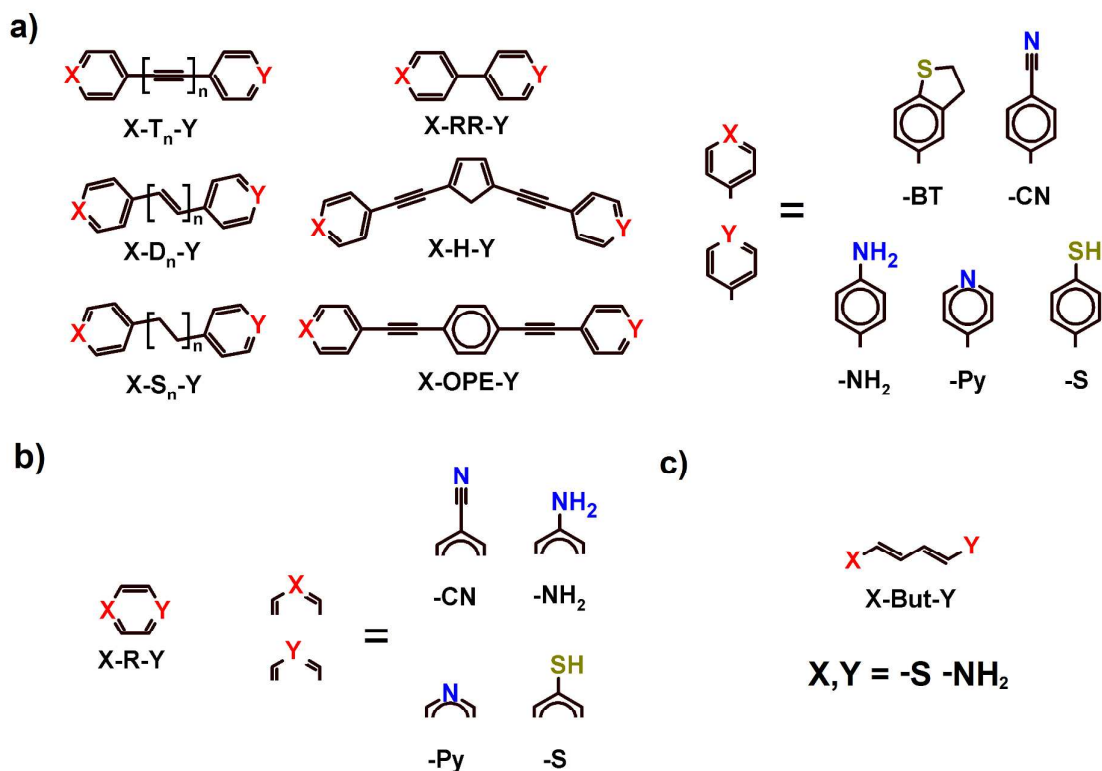


Figure 1. The 193 combinations of backbones and anchors used to obtain figure 2. a) The left column shows 3 alkanes, 3 alkenes and 3 alkynes (where $n=1,2,3$) and the second-from-left column shows 3 other backbones. (ie a total of 12 backbones). The right panel shows 5 anchors cyano (CN), pyridil (Py), dihidrbenzothiol (BT), amine (NH_2) and thiol(S). These combine to yield 12×5 symmetric molecules and $12 \times 5 \times 4 / 2 = 120$ asymmetric molecules (ie 180 molecules in total). b) Molecules with a single ring as the backbone and four kinds of anchors: in total there are 4 symmetric and 6 asymmetric variants of these (ie 10 in total). c) shows a single butadiene chain with two kinds of anchors: in total there is one symmetric and

two asymmetric versions of this. All of the molecular geometries are shown in the SI in Figures S1-S14.

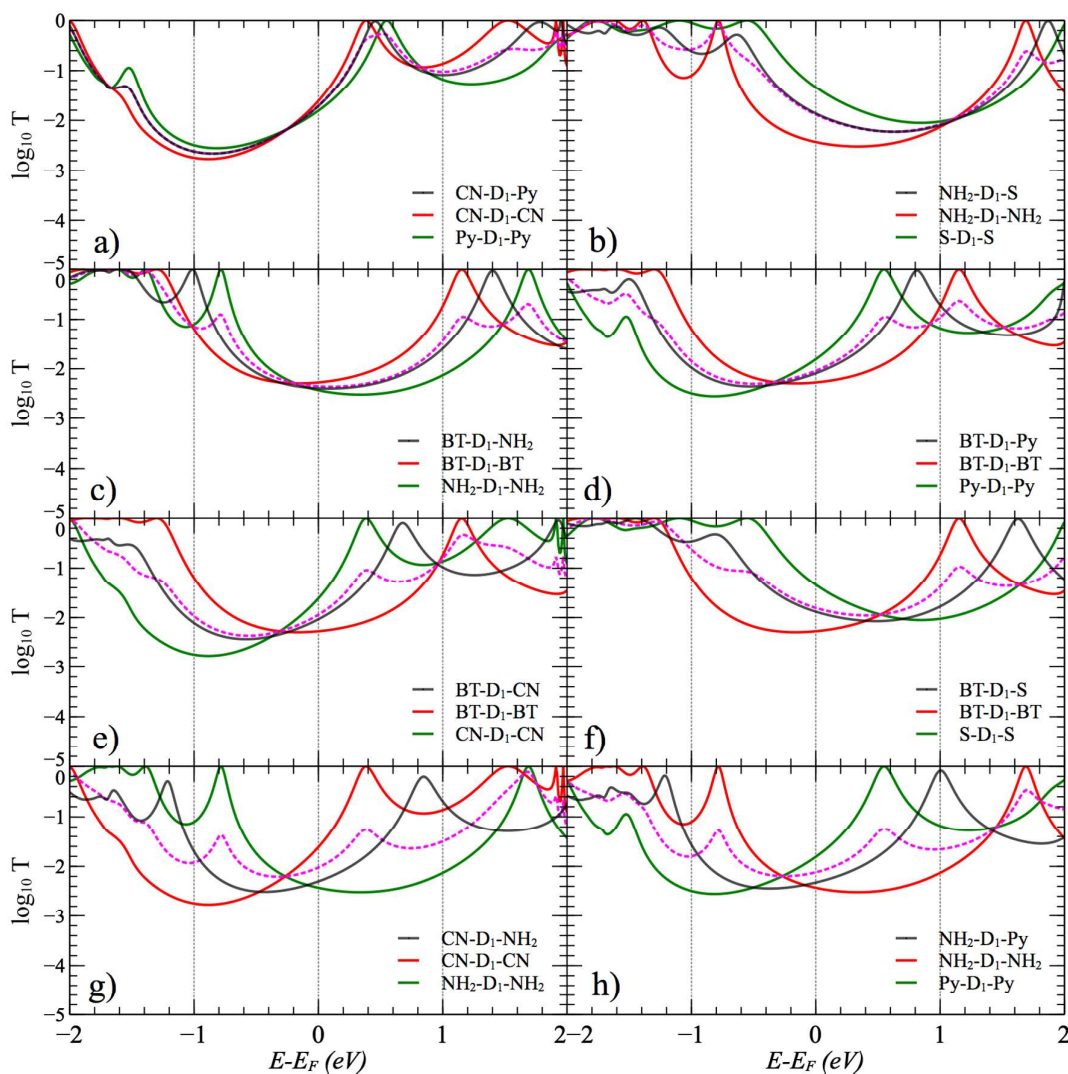


Figure 2. Transmission coefficients for symmetric and asymmetric molecules $X-D_1-X$, $Y-D_1-Y$ and $X-D_1-Y$. The dashed pink curves show the circuit rule predictions for $X-D_1-Y$. Choices of X , Y are: (a) CN, Py (b) NH_2 , S (c) BT, NH_2 (d) BT, Py (e) BT, CN (f) BT, S (g) CN, NH_2 (h) Py, NH_2 . Additional transmission coefficient curves are shown in the SI in Figures S15-S28.

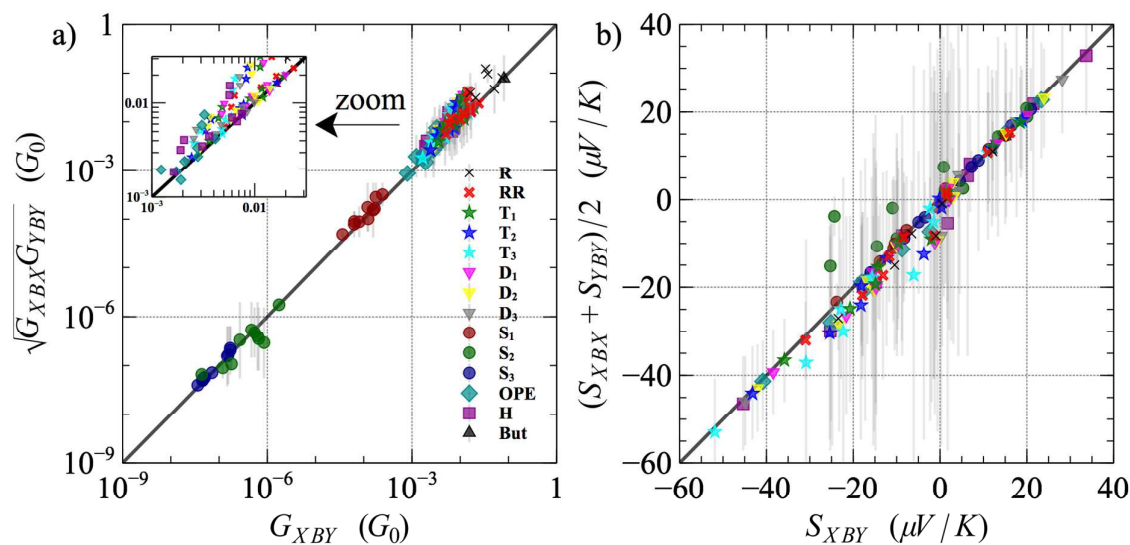


Figure 3. a) Comparison between the conductances G_{XBY} and the geometric means $(G_{XBx}G_{YBY})^{1/2}$. b) Comparison between the thermopowers S_{XBY} and the arithmetic means $(S_{XBx} + S_{YBY})/2$. The top and bottom ends of the vertical grey lines show the values for the symmetric molecules used in the circuit rules. The different colours and markers indicate the various molecular backbones. The notation in the legend is as follows the backbone labelling in Figure 1.

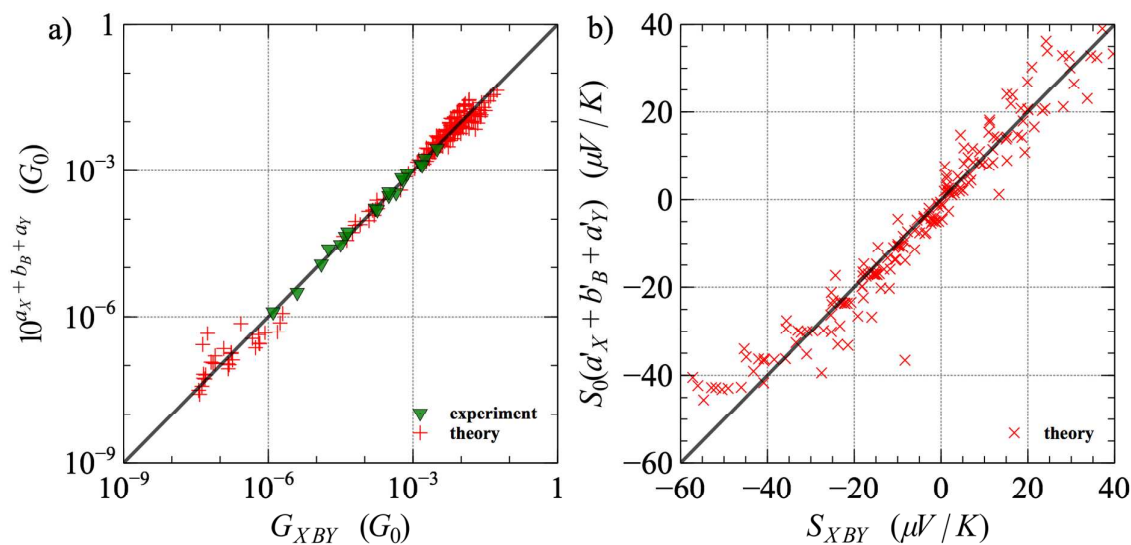


Figure 4. Factorized conductance and thermopower approximations are plotted against the DFT computed values (red markers) and experimental values (green triangles). In panel a), for each DFT-computed conductance G_{XBY} , a red cross marks the corresponding $10^{a_X + b_B + a_Y} G_0$ value. In panel b) for each DFT-computed thermopower S_{XBY} , a red cross marks the corresponding $(a'_X + b'_B + a'_Y) S_0$ value. In both cases the a_X, a'_X parameters and b_B, b'_B parameters are taken from Table 1. The green triangles in panel a) show the factorization of a selection of experimental conductances from the literature, quoted in Table 3. For each experimental conductance G_{XBY} the green triangle marks the corresponding $10^{a_X + b_B + a_Y} G_0$ value, where the a_X parameters and b_B parameters are taken from Table 2. $G_0 = 2e^2/h$. $S_0 = k_B/e$.

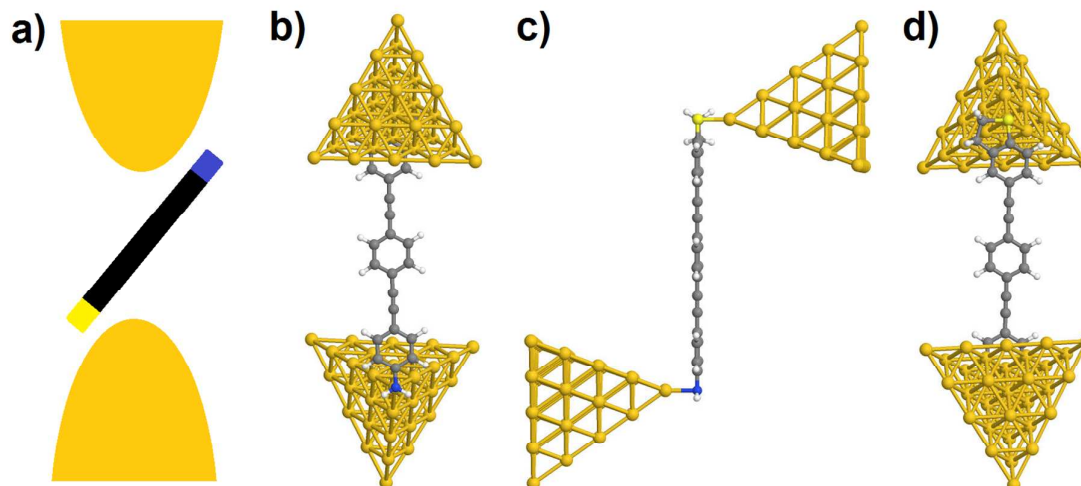


Figure 5. a) Molecule arrangement in break-junction experiment. b),c),d) Three views of the same junction. Top, side and bottom views, respectively, of the model junction geometry of a particular case (BT-OPE-NH₂) for systematic comparisons.

TABLES

Table 1 Anchor and backbone parameters obtained by fitting eqs. 3 and 4 to the DFT-computed room temperature conductances ($\log_{10}(G/G_0)$) and thermopowers (Se/k_B) respectively

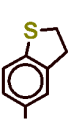
Anchor X with rings		 -BT	 -CN	 -NH ₂	 -Py	 -S
a_X		-1.12	-0.89	-1.20	-0.87	-0.68
a'_X		-0.02	-0.24	0.06	-0.17	0.19
Backbones B	RR	T ₁	T ₂	T ₃	OPE	H
b_B	0.00	-0.12	-0.25	-0.38	-0.73	-0.46
b'_B	0.00	-0.01	-0.05	-0.09	-0.02	0.01
Backbones B	D ₁	D ₂	D ₃	S ₁	S ₂	S ₃
b_B	-0.09	-0.22	-0.35	-2.04	-4.57	-5.19
b'_B	-0.01	-0.01	-0.01	0.03	0.06	0.10

Table 2 Anchor and backbone parameters obtained by fitting eq. 3 to the experimental room temperature conductance ($\log_{10}(G/G_0)$). For the $n_A=5$ anchor and $n_B=6$ backbone, the parameters give the

conductance of $n_A(n_A+1)n_B/2=90$ molecules in the form of $G_{XBY} = 10^{a_X+b_B+a_Y}G_0$.^(a) an example for this backbone is 'pmp' from ref²⁰.

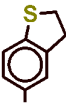
Anchor X with rigins						
		-BT	-CN	-NH ₂	-Py	-S
a_X (from experiments)	-	-1.12	-2.15	-1.44	-1.58	-1.22
Backbones B	RR	T ₁	T ₂	T ₄	OPE	OPE(meta) ^(a)
b_B (from experiments)	0.00	-0.31	-0.63	-1.20	-1.37	-2.75

Table 3 Comparison between experimental conductances and the computed conductances from equ. 3, using the fitted anchor and backbone parameters shown in table 2. Experimental values are taken from^(a) from ref⁴⁰ by averaging STM-BJ and MCBJ values, ^(b) from ref³¹, ^(c) from ref²⁰, ^(d) from ref²⁶, ^(e) from ref³⁹, ^(f) from ref²⁹.

Molecule X B Y	Experimental $\log_{10} \frac{G}{G_0}$	$a_X + b_B + a_Y$	Molecule X B Y	Experimental $\log_{10} \frac{G}{G_0}$	$a_X + b_B + a_Y$
Py T ₁ Py	-3.35 ^(a)	-3.47	CN T ₁ CN	-4.75 ^(a)	-4.61
Py T ₂ Py	-3.78 ^(a)	-3.79	CN T ₂ CN	-4.9 ^(a)	-4.93
Py T ₄ Py	-4.4 ^(a)	-4.36	CN T ₄ CN	-5.4 ^(a)	-5.50
NH ₂ T ₁ NH ₂	-3.205 ^(a)	-3.19	S T ₁ S	-2.75 ^(a)	-2.75
NH ₂ T ₂ NH ₂	-3.5 ^(a)	-3.51	S T ₂ S	-3.12 ^(a)	-3.07
BT T ₁ BT	-2.5 ^(a)	-2.55	Py OPE Py	-4.5 ^(c)	-4.53
BT T ₂ BT	-2.845 ^(a)	-2.87	S OPE S	-3.74 ^(d)	-3.81
BT T ₄ BT	-3.5 ^(a)	-3.44	NH ₂ OPE NH ₂	-4.35 ^(e)	-4.25
Py RR Py	-3.23 ^(b)	-3.15	Py OPE(meta) Py (pmp) ^(e)	-5.9 ^(c)	-5.91
NH ₂ RR NH ₂	-2.81 ^(f)	-2.89			

Table 4 Conductance predictions for a few new molecules based on Table 2. Predictions from Table 2 for all combinations of backbones and anchors are presented in Table S1 of the SI.

Molecule X B Y	$a_X + b_B + a_Y$ ($\log_{10}(G/G_0)$)	Molecule X B Y	$a_X + b_B + a_Y$ ($\log_{10}(G/G_0)$)
Py-T ₁ -CN	-4.04	Py-OPE-NH ₂	-4.39
Py-T ₁ -NH ₂	-3.33	Py-OPE-BT	-4.07
Py-T ₁ -BT	-3.01	Py-OPE-S	-4.17
Py-T ₁ -S	-3.11	CN-OPE-CN	-5.67
CN-T ₁ -NH ₂	-3.90	CN-OPE-NH ₂	-4.96
CN-T ₁ -BT	-3.58	CN-OPE-BT	-4.64
CN-T ₁ -S	-3.68	CN-OPE-S	-4.74
NH ₂ -T ₁ -BT	-2.87	NH ₂ -OPE-BT	-3.93
NH ₂ -T ₁ -S	-2.97	NH ₂ -OPE-S	-4.03
BT-T ₁ -S	-2.65	BT-OPE-BT	-3.61
Py-OPE-CN	-5.10	BT-OPE-S	-3.71

ASSOCIATED CONTENT

Supporting Information Available: Content includes figures for all molecular geometries and all computed transmission coefficient functions. Theoretical predictions for the conductance of all anchor group/backbone combinations are included in Table S1. This material is available free of charge via internet at <http://pubs.acs.org>.

AUTHOR INFORMATION

Corresponding Author

c.lambert@lancaster.ac.uk; d.manrique@lancaster.ac.uk;

Present Addresses

†If an author's address is different than the one given in the affiliation line, this information may be included here.

Author Contributions

DZM, WH and CJL conceived the research idea. The calculations were performed by DZM and QA and the manuscript has been prepared by DZM, QA and CJL. The manuscript was written through contributions of all authors. All authors have given approval to the final version of the manuscript.

Notes

The authors declare no competing financial interest.

ACKNOWLEDGMENTS

This work was generously supported by the UK EPSRC projects EP/N017188/1, EP/M014452/1, the EC FP7 ITN "MOLESCO" project number 606728, and the Higher Education Ministry, Al Qadisiyah University, IRAQ.

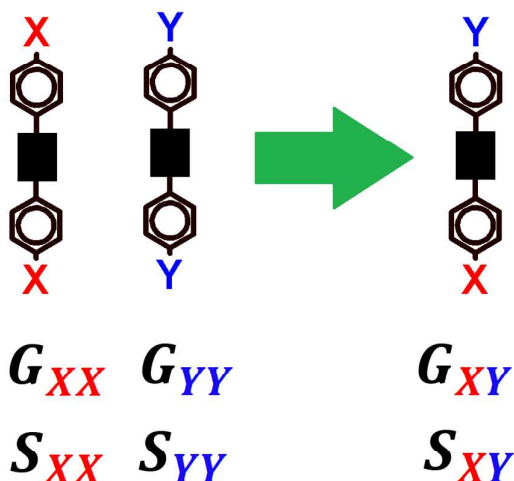
REFERENCES

- (1) Repp, J.; Meyer, G.; Paavilainen, S.; Olsson, F. E.; Persson, M. *Science* **2006**, 312, (5777), 1196-1199.
- (2) Donhauser, Z. J.; Mantooth, B. A.; Kelly, K. F.; Bumm, L. A.; Monnell, J. D.; Stapleton, J. J.; Price Jr., D. W.; Rawlett, A. M.; Allara, D. L.; Tour, J. M.; Weiss, P. S. *Science* **2001**, 292, 2303-2307.
- (3) Wold, D. J.; Haag, R.; Rampi, M. A.; Frisbie, C. D. *J. Phys. Chem. B* **2002**, 106, (11), 2813-2816.
- (4) Fan, F. R. F. *J. Am. Chem. Soc.* **2002**, 124, 5550-5560.
- (5) Widawsky, J. R.; Darancet, P.; Neaton, J. B.; Venkataraman, L. *Nano Lett.* **2012**, 12, (1), 354-358.
- (6) Venkataraman, L.; Klare, J. E.; Nuckolls, C.; Hybertsen, M. S.; Steigerwald, M. L. *Nat.* **2006**, 442, (7105), 904-907.
- (7) Hong, W.; Valkenier, H.; Meszaros, G.; Manrique, D. Z.; Mishchenko, A.; Putz, A.; Garcia, P. M.; Lambert, C. J.; Hummelen, J. C.; Wandlowski, T. *Beilstein J. Nanotechnol.* **2011**, 2, 699-713.
- (8) Seferos, D. S.; Trammell, S. A.; Bazan, G. C.; Kushmerick, J. G. *P. NATL. ACAD. SCI. USA* **2005**, 102, (25), 8821-8825.
- (9) Dadosh, T.; Gordin, Y.; Krahne, R.; Khivrich, I.; Mahalu, D.; Frydman, V.; Sperling, J.; Yacoby, A.; Bar-Joseph, I. *Nat.* **2005**, 436, (7054), 1200-1200.
- (10) Liao, J.; Bernard, L.; Langer, M.; Schonenberger, C.; Calame, M. *Adv. Mater.* **2006**, 18, (18), 2803-2804.
- (11) Reed, M. A.; Zhou, C.; Muller, C. J.; Burgin, T. P.; Tour, J. M. *Science* **1997**, 278, (5336), 252-254.
- (12) Park, J.; Pasupathy, A. N.; Goldsmith, J. I.; Chang, C.; Yaish, Y.; Petta, J. R.; Rinkoski, M.; Sethna, J. P.; Abruña, H. D.; McEuen, P. L. *Nat.* **2002**, 417, (6890), 722-725.
- (13) Osorio, E.; Bjørnholm, T.; Lehn, J.; Ruben, M.; Van der Zant, H. *J. Phys.: Condens. Matter* **2008**, 20, (37), 374121.
- (14) Chen, J.; Reed, M. A.; Rawlett, A. M.; Tour, J. M. *Science* **1999**, 286, 1550-1552.

- 1
2
3 (15) Aviram, A.; Ratner, M. *Chem. Phys. Lett.* **1974**, *29*, 277-283.
- 4 (16) Finch, C. M.; Sirichantaropass, S.; Bailey, S. W.; Grace, I. M.; García-Suárez, V. M.;
5 Lambert, C. J. *J. Phys.: Condens. Matter* **2008**, *20*, (2), 022203.
- 6 (17) Peterfalvi, C. G.; Grace, I.; Manrique, D. Z.; Lambert, C. J. *J. Chem. Phys* **2014**, *140*,
7 (17), 174711.
- 8 (18) Evangeli, C.; Gillemot, K.; Leary, E.; González, M. T.; Rubio-Bollinger, G.; Lambert,
9 C. J.; Agrait, N. *Nano Lett.* **2013**, *13*, (5), 2141-2145.
- 10 (19) Zhao, X.; Huang, C.; Gulcur, M.; Batsanov, A. S.; Baghernejad, M.; Hong, W.;
11 Bryce, M. R.; Wandlowski, T. *Chem. Mater.* **2013**, *25*, (21), 4340-4347.
- 12 (20) Manrique, D. Z.; Huang, C.; Baghernejad, M.; Zhao, X.; Al-Owaedi, O. A.; Sadeghi,
13 H.; Kaliginedi, V.; Hong, W.; Gulcur, M.; Wandlowski, T.; Bryce, M. R.; Lambert, C. J. *Nat.*
14 *Commun.* **2015**, *6*, 6389A, No. 8.
- 15 (21) Lambert, C. *Chem. Soc. Rev.* **2015**, *44*, (4), 875-888.
- 16 (22) Cuevas, J. C.; Scheer, E., *Molecular electronics: an introduction to theory and*
17 *experiment. World Scientific: 2010; Vol. 1.*
- 18 (23) Sparks, R.; García-Suárez, V. M.; Manrique, D. Z.; Lambert, C. J. *Phys. Rev. B* **2011**,
19 *83*, (7), 075437.
- 20 (24) Finch, C. M.; Garcia-Suarez, V. M.; Lambert, C. J. *Phys. Rev. B* **2009**, *79*, (3),
21 033405.
- 22 (25) Hong, W.; Manrique, D. Z.; Moreno-Garcia, P.; Gulcur, M.; Mishchenko, A.;
23 Lambert, C. J.; Bryce, M. R.; Wandlowski, T. *J. Am. Chem. Soc.* **2012**, *134*, (4), 2292-2304.
- 24 (26) Kaliginedi, V.; Moreno-García, P.; Valkenier, H.; Hong, W.; García-Suárez, V. M.;
25 Buitter, P.; Otten, J. L. H.; Hummelen, J. C.; Lambert, C. J.; Wandlowski, T. *J. Am. Chem.*
26 *Soc.* **2012**, *134*, (11), 5262-5275.
- 27 (27) Yoshida, K.; Pobelov, I. V.; Manrique, D. Z.; Pope, T.; Meszaros, G.; Gulcur, M.;
28 Bryce, M. R.; Lambert, C. J.; Wandlowski, T. *Sci. Rep.* **2015**, *5*, 9002A, No. 8.
- 29 (28) Mishchenko, A.; Zotti, L. A.; Vonlanthen, D.; Buerkle, M.; Pauly, F.; Carlos Cuevas,
30 J.; Mayor, M.; Wandlowski, T. *J. Am. Chem. Soc.* **2011**, *133*, (2), 184-187.
- 31 (29) Hybertsen, M. S.; Venkataraman, L.; Klare, J. E.; Cwhalley, A.; Steigerwald, M. L.;
32 Nuckolls, C. *J. Phys.: Condens. Matter* **2008**, *20*, (37), 374115.
- 33 (30) Quek, S. Y.; Venkataraman, L.; Choi, H. J.; Louie, S. G.; Hybertsen, M. S.; Neaton, J.
34 B. *Nano Lett.* **2007**, *7*, (11), 3477-3482.
- 35 (31) Quek, S. Y.; Kamenetska, M.; Steigerwald, M. L.; Choi, H. J.; Louie, S. G.;
36 Hybertsen, M. S.; Neaton, J. B.; Venkataraman, L. *Nat. Nanotechnol.* **2009**, *4*, (4), 230-234.
- 37 (32) Kanthasamy, K.; Pfnuer, H. *Beilstein J. Nanotechnol.* **2015**, *6*, 1690-1697.
- 38 (33) Egger, D. A.; Liu, Z.-F.; Neaton, J. B.; Kronik, L. *Nano Letters* **2015**, *15*, (4), 2448-
39 2455.
- 40 (34) Jin, C.; Strange, M.; Markussen, T.; Solomon, G. C.; Thygesen, K. S. *J. Chem. Phys.*
41 **2013**, *139*, (18), 184307.
- 42 (35) Quek, S. Y.; Khoo, K. H. *Acc. Chem. Res.* **2014**, *47*, (11), 3250-3257.
- 43 (36) Berritta, M.; Manrique, D. Z.; Lambert, C. J. *Nanoscale* **2015**, *7*, (3), 1096-1101.
- 44 (37) Wang, K.; Zhou, J.; Hamill, J. M.; Xu, B. *J. Chem. Phys.* **2014**, *141*, (5), 054712.
- 45 (38) Baghernejad, M.; Manrique, D. Z.; Li, C.; Pope, T.; Zhumaev, U.; Pobelov, I.;
46 Moreno-Garcia, P.; Kaliginedi, V.; Huang, C.; Hong, W.; Lambert, C.; Wandlowski, T.
47 *Chem. Commun.* **2014**, *50*, (100), 15975-15978.
- 48 (39) Gonzalez, T. M.; Zhao, X.; Manrique, D. Z.; Miguel, D.; Leary, E.; Gulcur, M.;
49 Batsanov, A. S.; Rubio-Bollinger, G.; Lambert, C. J.; Bryce, M. R.; Agrait, N. *J. Phys.*
50 *Chem. C* **2014**, *118*, (37), 21655-21662.
- 51
52
53
54
55
56
57
58
59
60

- (40) Moreno-Garcia, P.; Gulcur, M.; Manrique, D. Z.; Pope, T.; Hong, W.; Kaliginedi, V.; Huang, C.; Batsanov, A. S.; Bryce, M. R.; Lambert, C.; Wandlowski, T. *J. Am. Chem. Soc.* **2013**, 135, (33), 12228-12240.
- (41) Kim, T.; Darancet, P.; Widawsky, J. R.; Kotiuga, M.; Quek, S. Y.; Neaton, J. B.; Venkataraman, L. *Nano Lett.* **2014**, 14, (2), 794-798.
- (42) Sedghi, G.; García-Suárez, V. M.; Esdaile, L. J.; Anderson, H. L.; Lambert, C. J.; Martín, S.; Bethell, D.; Higgins, S. J.; Elliott, M.; Bennett, N. *Nat. Nanotechnol.* **2011**, 6, (8), 517-523.
- (43) Sangtarash, S.; Huang, C.; Sadeghi, H.; Sorohhov, G.; Hauser, J. r.; Wandlowski, T.; Hong, W.; Decurtins, S.; Liu, S.-X.; Lambert, C. J. *J. Am. Chem. Soc.* **2015**, 137, (35), 11425-11431.
- (44) Geng, Y.; Sangtarash, S.; Huang, C.; Sadeghi, H.; Fu, Y.; Hong, W.; Wandlowski, T.; Decurtins, S.; Lambert, C. J.; Liu, S.-X. *J. Am. Chem. Soc.* **2015**, 137, (13), 4469-4476.
- (45) Stewart, J. J. P. *J. Mol. Model.* **2013**, 19, (1), 1-32.
- (46) Huang, C. C.; Rudnev, A. V.; Hong, W. J.; Wandlowski, T. *Chem. Soc. Rev.* **2015**, 44, (4), 889-901.
- (47) Soler, J. M.; Artacho, E.; Gale, J. D.; García, A.; Junquera, J.; Ordejón, P.; Sánchez-Portal, D. *J. Phys.: Condens. Matter.* **2002**, 14, (11), 2745.
- (48) Ferrer, J.; Lambert, C. J.; Garcia-Suarez, V. M.; Manrique, D. Z.; Visontai, D.; Oroszlany, L.; Rodriguez-Ferradas, R.; Grace, I.; Bailey, S. W. D.; Gillemot, K.; Sadeghi, H.; Algharagholi, L. A. *New J. Phys.* **2014**, 16, 093029.
- (49) Verzijl, C. J. O.; Seldenthuis, J. S.; Thijssen, J. M. *J. Chem. Phys.* **2013**, 138, (9), 094102.

TABLE OF CONTENT GRAPHICS



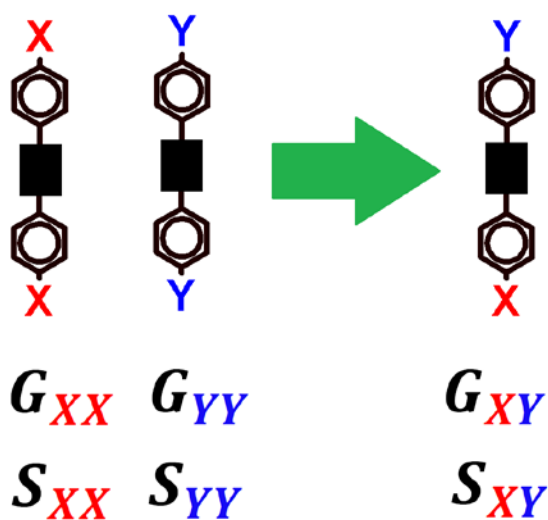
Conductance

$$G_{XY} = \sqrt{G_{XX}G_{YY}}$$

Thermopower

$$S_{XY} = \frac{S_{XX} + S_{YY}}{2}$$

TABLE OF CONTENT GRAPHICS

**Conductance**

$$G_{XY} = \sqrt{G_{XX}G_{YY}}$$

Thermopower

$$S_{XY} = \frac{S_{XX} + S_{YY}}{2}$$